JACS
JOURNAL OF THE AMERICAN CHEMICAL SOCIETY

Article

pubs.acs.org/JACS

Turning Supramolecular Receptors into Chemosensors by Nanoparticle-Assisted "NMR Chemosensing"

Marie-Virgine Salvia,[†,‡] Giovanni Salassa,[‡] Federico Rastrelli,[*] and Fabrizio Mancin[*]

Dipartimento di Scienze Chimiche, Università di Padova, via Marzolo 1, Padova, Italy

Supporting Information

ABSTRACT: By exploiting a magnetization transfer between monolayer-protected nanoparticles and interacting analytes, the NMR chemosensing protocol provides a general approach to convert supramolecular receptors into chemosensors via their conjugation with nanoparticles. In this context, the nanoparticles provide the supramolecular receptor not only with the "bulkiness" necessary for the NMR chemosensing approach but also with a different selectivity as compared to the parent receptor. We here demonstrate that gold nanoparticles of 1.8 nm core coated with a monolayer of 18-crown-6 ether derivatives can detect and identify protonated primary amines in methanol and in water, and even discriminate between two biogenic diamines that are selectively detected over monoamines and α-amino acids.

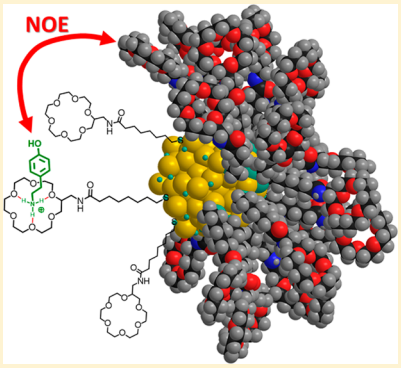

INTRODUCTION

Three decades after their introduction, chemosensors are still attracting great attention from a scientific and technological perspective.[1] Also known as "molecular chemical sensors", they are defined as molecular systems capable of detecting a target analyte by producing a measurable signal.[1a,2] The success encountered by such systems is mainly related to their flexibility, which has allowed their use in test kits and sensors, as well as in probes for intracellular and even *in vivo* detection of selected compounds.[3]

Generally, chemosensors are composed by two subunits: a receptor, which recognizes the analyte, and a signaling unit, which produces the output signal.[1a−c,4] These two units become a chemosensor *only* if a suitable *transduction mechanism* is active.[4] This mechanism converts the analyte recognition by the receptor into an observable property (namely, a physicochemical modification) of the signaling unit, and its design represents the major problem that must be addressed when a new chemosensor is conceived.[5]

In many examples, the transduction mechanism is based on the chemical properties of the analyte (chemical reactivity, photophysical properties, redox activity) that can induce a modification of the sensor properties.[1] In these cases, however, the sensing strategy cannot be generally transferred from one class of substrates to a new one. The realization of a chemosensor for a different analyte requires consequently a nonstraightforward design and optimization procedure.

In order to make the chemosensor design simpler, several strategies have been proposed over the years to provide general transduction mechanisms that can be implemented in any system, and the demand for such strategies is still high.

The so-called "intrinsic" approach[1a] used in the first chemosensors[6] already belonged to this category. In these systems, where signaling is based on the change in the light absorption or emission properties of the chemosensor, the receptor is designed in such a way as to be integrated into the chromophoric (signaling) unit. Hence, the binding of the analyte intrinsically modifies the state of the signaling units in order to generate the signal. Such a strategy however is not free from limitations: the strength and the extent of the interaction between the recognized analyte and the signaling units is difficult to predict or to extend from one analyte to another. Consequently, the effectiveness of the sensing systems can be lower than expected.

Such a limitation was first overcome by the photoinduced electron transfer (PET) luminescent sensors.[7] In this case, a luminescence self-quenching process, due to a photoinduced electron transfer from an electron rich moiety to the fluorogenic unit, is built into the sensor. The binding of the analyte decreases the availability of electrons for the photo-induced transfer and this restores the luminescence. Such a strategy is quite effective for detection of metal ions yet more difficult to apply to organic molecules.

The conformational modifications caused by substrate binding provide another useful sensing strategy, particularly in the case of fluorescent systems. If such modifications are well-defined and relevant enough, they can cause a substantial distance change between the interacting part of the sensors generating the signal. Examples of this strategy include activation/deactivation of FRET (Forster energy transfer) or quenching mechanisms.[8] Molecular beacons represent a very successful example of this approach.[9] These systems are DNA probes that report the presence of a specific target via a change

Received: June 17, 2015
Published: August 27, 2015

DOI: 10.1021/jacs.5b06300
J. Am. Chem. Soc. 2015, 137, 11399−11406

in conformation (i.e., from a hairpin to a double strand structure) triggered by hybridization or by a specific recognition event.

Another general chemosensing approach is the signaling unit displacement, also known as indicator displacement assay (IDA).[10] In this method, the signaling unit is an independent molecule noncovalently bound to the receptor unit. The complexation of the substrate by the receptor causes the displacement of the signaling unit, which is released in the solution and undergoes a consequent variation of its properties. Initially developed and highly successful for fluorescent chemosensors, this method has found application also in chromogenic and recently even in NMR-based chemosensors.[11] The noncovalent nature of the interaction between the receptor and the signaling unit limits however its application to "in tube" analyses, where dilution and a consequent spontaneous dissociation of the sensing complex are not possible.

In the case of metal ions, the problem has been solved by the "ion selective optode" approach.[12] Here, a neutral ionophore and a pH sensitive probe are merged into a hydrophobic matrix. The binding of the metal ion induces the deprotonation of the dye (to maintain the electroneutrality) and the consequent modification of its absorption/emission. Evidently, this sensing scheme only works with charged analytes.

NMR spectroscopy has recently emerged as an interesting alternative to optical spectroscopy and potentiometry, that are most commonly used for sensing applications. Several examples of relaxivity-based chemosensors for the detection of metal ions have been reported. These probes, which can be used for *in vivo* applications, are designed in such a way that the substrate binding alters the longitudinal relaxation time of water interacting with a Gd(III) contrast agent.[13]

^{19}F NMR has also attracted considerable attention. In fact, in addition to the high receptivity of ^{19}F, most organic compounds do not bear fluorine atoms in their structure, and ^{19}F spectra of a mixture under analysis contain typically a small number of signals arising only from the chemosensor. Swager and co-workers have recently demonstrated that the chemical shifts of fluorine atoms judiciously positioned in cavitand-type receptors can change by a different extent depending on the nature of the bound substrate. In this way, the chemosensor produces different signals for each substrate, thus allowing for detection and identification of the analyte.[14,15]

Our interest in the structure and interactions of monolayer protected nanoparticles investigated by NMR spectroscopy[16] has recently led us to report a new detection protocol, named "NMR chemosensing" (Scheme 1), based on the combined use of monolayer-protected gold nanoparticles (AuNP) and NMR.[17] The rationale of this method rests upon the slow diffusion rate of the nanoparticles with respect to small analytes, and on the intermolecular dipolar interactions as a pathway to transfer magnetization between two interacting species. Inspired by Shapiro's NOE pumping sequence,[18] the NMR chemosensing experiment starts with a diffusion filter which dephases the magnetization of all the small, fast diffusing species in the sample while retaining that of the nanoparticles. This magnetization is then transferred via NOE to the small analytes interacting with the nanoparticle monolayer, and the resulting signals are detected. The main advantage in the use of such nanoparticle-assisted spectral editing is the fact that the signal produced by the sensing system is the *full NMR spectrum of the analyte*, and not just a variation of one sensor property. This allows not only a detection and quantification of the analyte but also its unambiguous identification. Moreover, even unknown compounds or interferents detected by the sensing system may be, in principle, identified.

Scheme 1. Outline of the NMR Chemosensing Experiment[a]

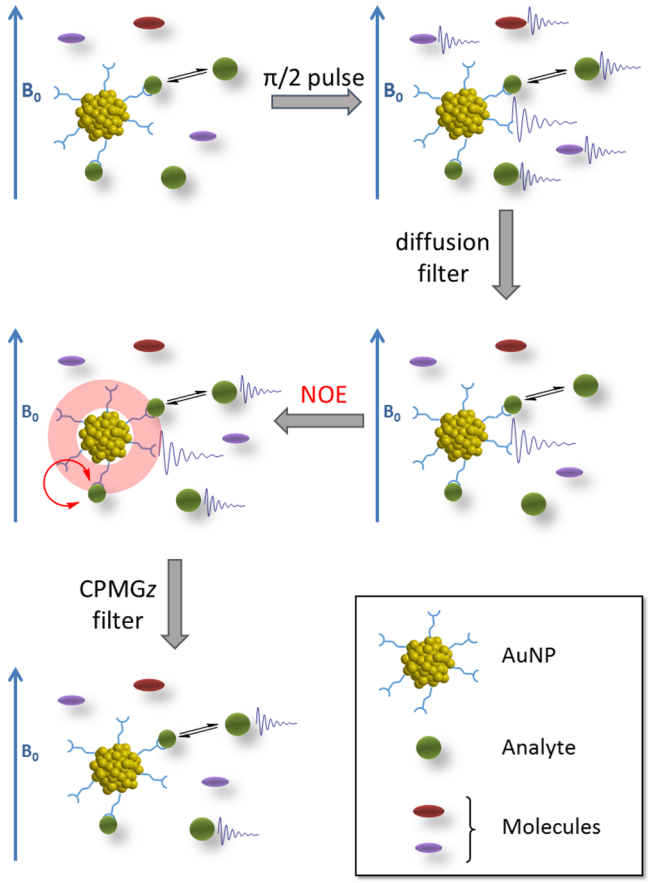

[a]A FID denotes the existence of observable signals after each pulse sequence block. The different sizes of the analyte molecules represent the unbalance between populations of the free and bound states. Details on the pulse sequence and CPMGz filter are provided in the Supporting Information and in ref 11a, respectively.

In this communication, we show that NMR chemosensing also provides a very general strategy for turning supramolecular receptors into chemosensors by their simple grafting to nanoparticles. In our previous examples, the analyte interaction with the nanoparticles was a micelle-like adsorption or inclusion into the nanoparticle coating monolayer, induced by hydrophobic and/or ion pairing interactions.[17] Albeit quite effective, such an interaction is not expected to provide high selectivity when comparted to the state of the art receptors used for molecular recognition. However, most supramolecular receptors are likely not suitable for NMR chemosensing. Indeed, the selection of receptors' NMR signals with a diffusion filter is not generally possible, since the receptor size (and hence its diffusion coefficient) is similar to that of the analytes. On this basis, we reasoned that conjugation of the same supramolecular receptor with a nanoparticle could result in a reduced diffusion rate, thus recovering the necessary condition for NMR chemosensing.

To prove this idea, we here report how crown ethers, selected as representative supramolecular receptors, can be turned into NMR chemosensors for amines by simply conjugating them with monolayer protected nanoparticles.[19]

DOI: 10.1021/jacs.5b06300
J. Am. Chem. Soc. 2015, 137, 11399−11406

Moreover, the spontaneous formation of multivalent binding sites on the particle surface provides the system with a selectivity different from that of the original receptor.

RESULTS AND DISCUSSION

The Detection System. 18-Crown-6 is well-known for its ability to bind ammonium and protonated primary amines by the formation of three $NH^+ \cdot O$ hydrogen bonds with the oxygen atoms in the 1, 7, and 13 positions.[20] For this reason, we selected it as a recognition unit for the development of a nanoparticle-based NMR chemosensor for protonate primary amines. Thiol **1** (Chart 1), bearing a 18-crown-6 moiety, was straightforwardly synthesized from commercially available 2-aminomethyl-18-crown-6. Gold nanoparticles with a 1.8 nm gold core protected with a monolayer of **1** (**1**-AuNP) were prepared by a two-phase, two-step method.[21]

Chart 1. Nanoparticle Passivating Thiol 1 and Substrates 2–10 Used in This Work

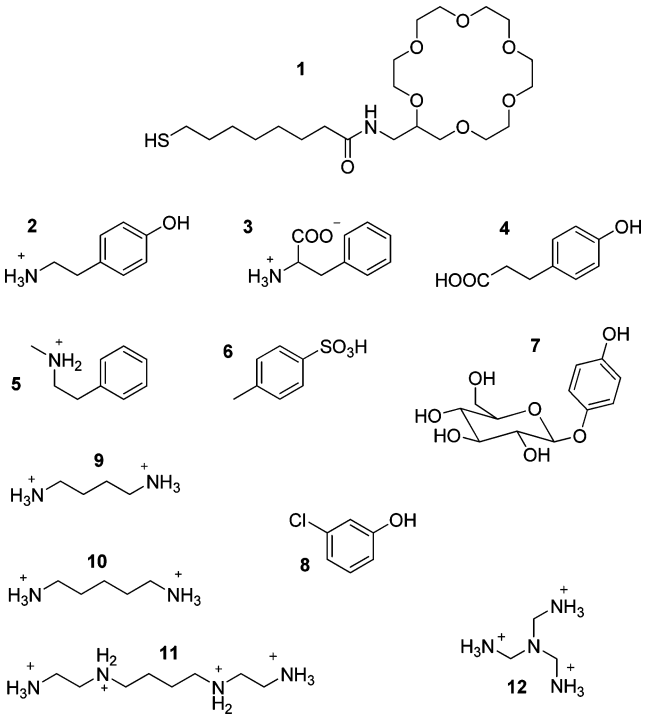

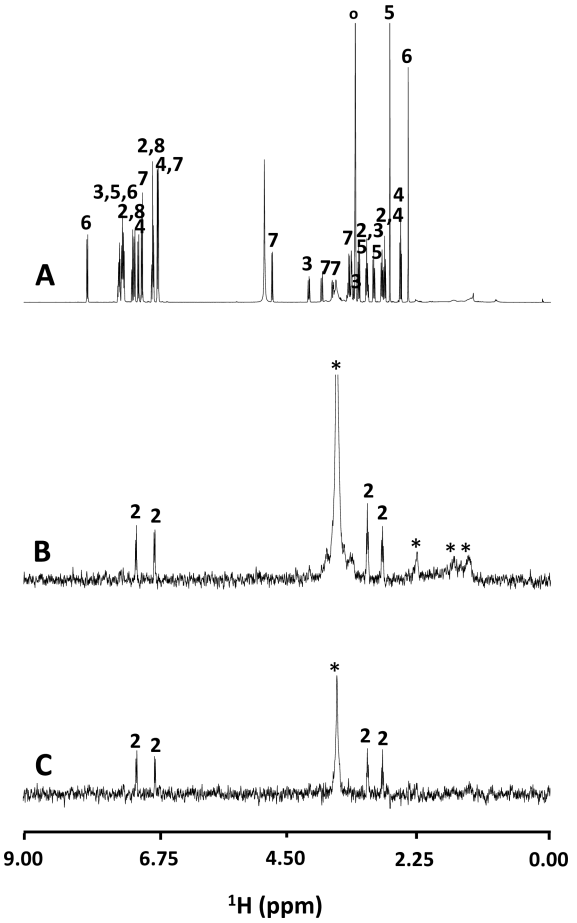

Figure 1. (A) ^{1}H NMR spectrum of a mixture of compounds **2**–**8**, each at 10 mM in CD_3OD. (B) NOE pumping spectrum of the same mixture in the presence of **1**-AuNP (29 μM). (C) The NOE pumping-CPMGz spectrum of the same mixture in the presence of **1**-AuNP (29 μM). (* = nanoparticles' residual signal, ° = residual solvents and impurities).

In the first step, the gold nanoparticles are formed by $NaBH_4$ reduction of $AuCl_4^-$ in toluene in the presence of tetraocylammonium bromide as a phase transfer catalyst and dioctylamine as a weak nanoparticle stabilizing agent. The thiol monolayer is subsequently formed by substitution of the dioctylamine monolayer with thiol **1**. The nanoparticles coated with **1** were soluble in water and methanol.

Once obtained, **1**-AuNPs were tested for their ability to detect protonated primary amines. Figure 1A,B illustrates the results of a NOE pumping experiment performed using **1**-AuNP (29 μM, corresponding to [**1**] = 2.0 mM)[22] and a mixture of (Chart 1) tyramine hydrochloride (**2**), phenylalanine (**3**), phloretic acid (**4**), *N*-methylphenethylamine hydrochloride (**5**), *p*-toluic acid (**6**), arbutin (**7**), and 3-chlorophenol (**8**) each 10 mM in CD_3OD. Inspection of Figure 1A clearly reveals the difficulties one may encounter in using NMR for analyzing mixtures of compounds. Several signals are present in the ^{1}H NMR spectrum with some overlapping, and assignment of the sets of signals arising from a single compound, even if well resolved, is not trivial. The compounds in this mixture possess several functional groups which may potentially interact with the nanoparticle coating monolayer via H-bonding. This challenging situation allows us to test both the chemical selectivity of the sensing system and its spectroscopic ability to discriminate overlapping signals at the same time.

Remarkably, only the tyramine signals are observed in the NOE pumping spectrum reported in Figure 1B, allowing its unambiguous identification in the original mixture. This result clearly indicates that the grafting of 18-crown-6 to small nanoparticles results in a sensing system highly selective for protonated primary amines.

Interestingly, the selectivity of the nanoparticle-based system is even greater than that of the parent receptor. Indeed, not only compounds without the protonated primary amino group, as **4**, **6**, **7**, **8**, and **5**,[24] but even α-amino acids, as **3**, are not detected in the nanoparticle assisted NOE pumping spectrum. The strength of the ammonium–crown ether interaction is very sensitive to steric effects (see infra).[20a] The low affinity revealed here by the nanoparticle system for α-amino acids could be ascribed to this property. It may be expected that the crowding of crown ether moieties on the particle surface amplifies the

DOI: 10.1021/jacs.5b06300
J. Am. Chem. Soc. 2015, 137, 11399–11406

sensitivity to steric effects as those likely arising from the substituents of the carbon in α.

In order to give a full account of the potential of this approach, we tried to analyze the mixture with other methods usually applied to NMR analysis of mixtures (see the Supporting Information). Remarkably, DOSY, selective TOCSY, and saturation transfer difference (STD) experiments (the latter in the presence of **1**-AuNPs) failed in clearly identifying the presence of **2** in the mixture (Figures S5−S7). The reason for the failure can be attributed to signal overlap (STD),[25] too similar diffusion rates (DOSY), or a break in the analyte's spin systems (TOCSY). In the end, nanoparticle-assisted NOE pumping emerges as the only general technique allowing the full and unambiguous identification of an analyte interacting selectively with the nanoparticles in a complex mixture.

Inspection of Figure 1B reveals however one relevant limitation of the NMR chemosensing experiments performed with the standard NOE pumping pulse sequence.[17b] Namely, the final NMR spectrum contains not only the signals of the analyte interacting with the nanoparticles but also the signals of the nanoparticles themselves (in much the same way as diagonal peaks are found in a 2D NOESY spectrum). Since the nanoparticle signals have an intensity comparable to (or even larger than) those of the analytes, their presence in the final spectrum could potentially interfere with the analyte identification.

In some cases, this problem can be partially addressed by optimizing the duration of the NOE mixing time to exploit the exponential decay of the nanoparticle signals, as opposed to the NOE buildup of the analyte signals (namely, an initial increase followed by a decrease at long mixing times, Figure 2).

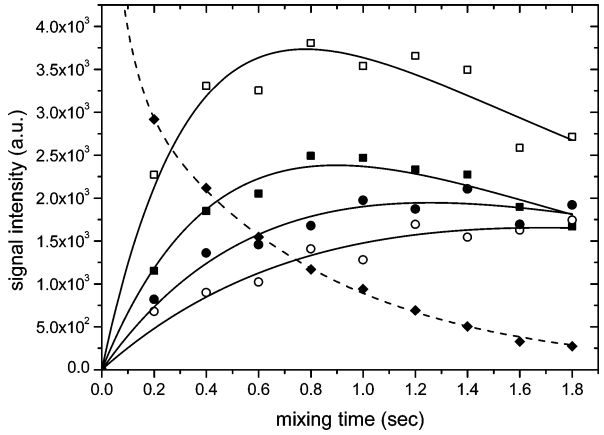

Figure 2. NOE buildup evolution of tyramine hydrochloride (**2**) signals (■ = H_c, 2.9 ppm; □ = H_d, 3.1 ppm; ○ = H_a, 6.8 ppm; ● = H_b, 7.1 ppm) and decay of a selected **1**-AuNP signal (◆, 3.66 ppm, intensity divided by 10) in CD_3D. Conditions: [**2**] = 10 mM, [**1**-AuNP] = 29 μM, T = 25 °C. Lines represent the best fit of the data according to the transient NOE model.[23]

However, such a solution is not of general applicability, since the maximum intensity for the analyte signals may be reached at mixing times where the intensity of the nanoparticle signals is still significant (Figure 2).

In order to circumvent this limitation, we tried to take advantage of the fast transverse relaxation typical of the nanoparticle spins, which endows an efficient T_2-filtration just before signal detection. In this way, the residual nanoparticle signals (having short T_2) are removed from the spectrum, while those of the analyte (featuring longer T_2) are retained. To this scope, the CPMG*z* pulse scheme[16a] is particularly suitable, as it requires no phase cycling to produce clean spectra. The advantages of appending a CPMG*z* filter to the NOE pumping pulse scheme are evident by comparing parts B and C of Figure 1. In the latter, the nanoparticle signals have been significantly reduced or even completely removed, and the spectrum of **2** can be easily identified.

Taken together, the above results confirm that 18-crown-6 is turned into a NMR chemosensor, capable of detecting and identifying protonated primary amines, by conjugation with the gold nanoparticle. In principle, such a strategy can be extended to any supramolecular receptor capable of recognizing organic molecules.

Multivalent Binding. In order to confirm that the analyte detection comes from a molecular recognition of the primary ammonium group by the crown ether receptor (and not by unspecific absorption), we investigated the interaction between **2** and **1**-AuNP in more detail. The first evidence arises from a deeper analysis of the NOE pumping spectra in Figure 1B and C, which reveals that the signals of the alkyl protons are larger than those of the aromatic protons. This qualitative information is confirmed by inspection of Figure 2, which highlights that the NOE buildup is faster for aliphatic than for aromatic protons. Whenever intramolecular dipolar interactions are modulated during the lifetime of the complex, faster NOE buildups are generally expected on substrate protons lying closer to the receptor. Albeit spin diffusion and relay effects may complicate a quantitative analysis, the behavior observed for cross relaxation rates of **2** is consistent with an interaction that drives the alkylammonium portion of **1** closer to the nanoparticle monolayer than the aromatic part, as expected in a typical crown ether−ammonium interaction.

Further evidence of the substrate recognition mechanism was obtained by repeating the experiment (Figure 3) in the presence of the strong organic base DBU (1,8-diazabicyclo-[5.4.0]undec-7-ene). In this case, tyramine signals are not visible in the NOE pumping spectrum (Figure 3C,D). The deprotonation of the ammonium groups by DBU reduces both the number and the strength of the hydrogen bonds that tyramine can form with 18-crown-6, which ultimately decreases the binding of the substrate to the nanoparticles.[20a]

Other insight into the features of the receptor−substrate interaction was obtained by investigating the detection of protonated diamines. In this case, we applied the NOE pumping experiment to samples containing **1**-AuNP along with putrescine (**9**) or cadaverine (**10**) in their protonated form (Figure 4). These molecules are biologically relevant diamines differing only in the linear alkyl chain length connecting the two amino groups, with **10** being longer by one carbon atom. Most supramolecular chemosensors for chromogenic diamines produce similar signals for both substrates, even when they recognize them with different affinity.[20c,26] On the other hand, the two molecules can be easily distinguished by NMR chemosensing thanks to the differences in their ^{1}H spectra. Indeed, inspection of Figure 4 confirms that both the molecules are recognized and revealed by **1**-AuNP. However, the presence of the diagnostic signal at 1.6 ppm (relative to protons ***c*** of the alkyl chain) in the spectrum of **10** (Figure 4C, left side) easily allows its identification. In this case, the use of the NOE pumping-CPMG*z* sequence is essential, since the residual nanoparticle signals found in the standard NOE pumping

DOI: 10.1021/jacs.5b06300
J. Am. Chem. Soc. 2015, 137, 11399−11406

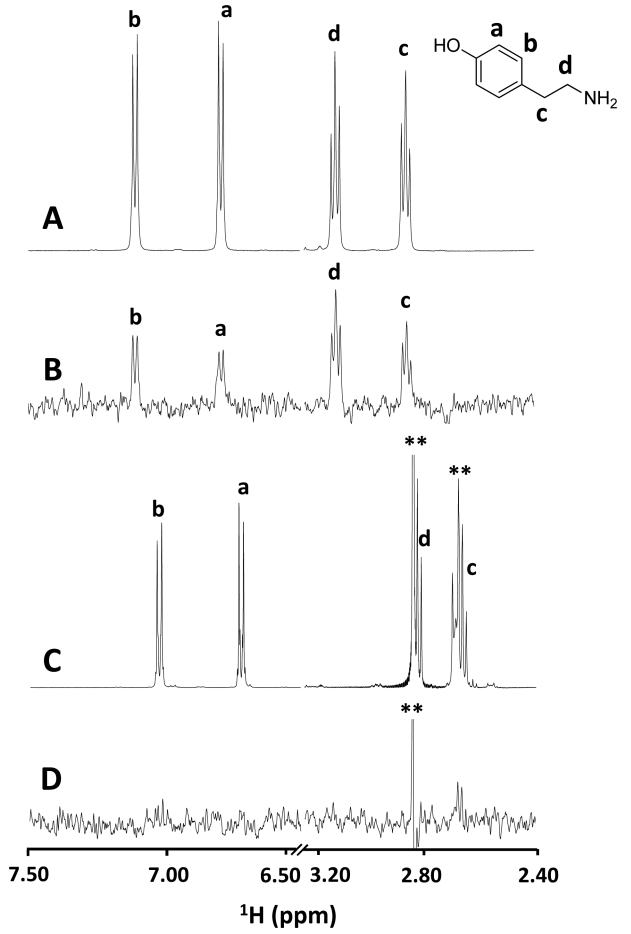

Figure 3. (A) ^{1}H NMR spectrum of **2** (10 mM in MeOD). (B) NOE pumping spectrum of **2** in the presence of **1**-AuNP (29 μM). (C) ^{1}H NMR spectrum of **2** (10 mM in CD_3OD) in the presence of diazabicyclo[5.4.0]undec-7-ene (DBU, **, 10 mM). (D) NOE pumping spectrum of **2** in the presence of **1**-AuNP (29 μM) and DBU.

spectrum mask the 1.6 ppm diagnostic signal of cadaverine (Figure 4B, left side).

The nanoparticle affinity for the two molecules, as well as for tyramine hydrochloride (**2**), was determined by combined titration and NOE pumping experiments (Figure 5). In all cases, the integrated intensities of the analyte signals increase with the concentration following a saturation profile. As we previously demonstrated, such binding profiles can be used as calibration curves for the analyte detection.[17a] A fit of the integrated signal intensities versus the analyte concentration with a 1:1 binding model provided an apparent association constant (K_{assoc}) value of 1.6×10^2 M^{-1} for **2**. Moreover, a detection limit of 3.8 mM could be determined, defined as the smallest substrate concentration of **2** producing a signal intensity 3 times larger than the standard deviation of the noise.[27] The K_{assoc} value obtained is at least 1 order of magnitude smaller than those reported for the binding of protonated primary amines to 18-crown-6.[20] As in the case of α-amino acids previously discussed, this effect also can be ascribed to the sensitivity of the crown ether−primary ammonium interaction to steric effects and to the crowding of crown ether moieties on the particle surface, which could prevent the optimal accommodation of the substrate.

In the case of **9** and **10**, two binding modes are possible, involving respectively the interaction of the protonated

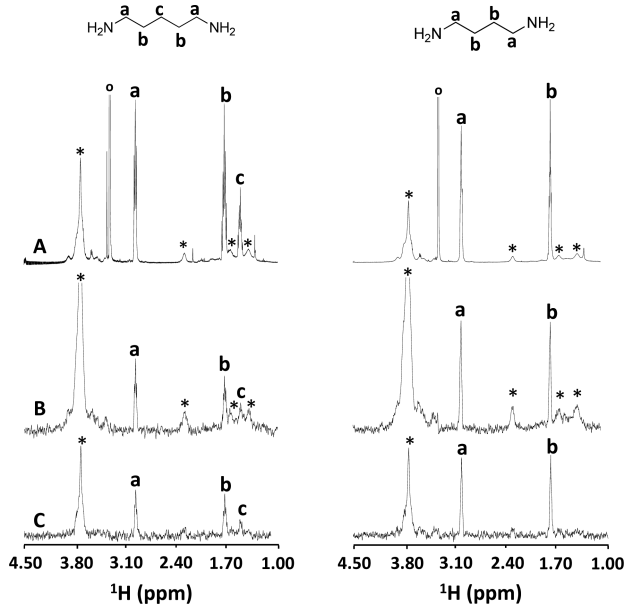

Figure 4. (A) ^{1}H NMR spectra of putrescine **9** (right) and cadaverine **10** (left) each 10 mM in CD_3OD. (B) NOE pumping spectra of **9** and **10** in the presence of 29 μM **1**-AuNP. (C) NOE pumping-CPMGz spectra of **9** and **10** in the presence of 29 μM **1**-AuNP (60 ms CPMGz filter).

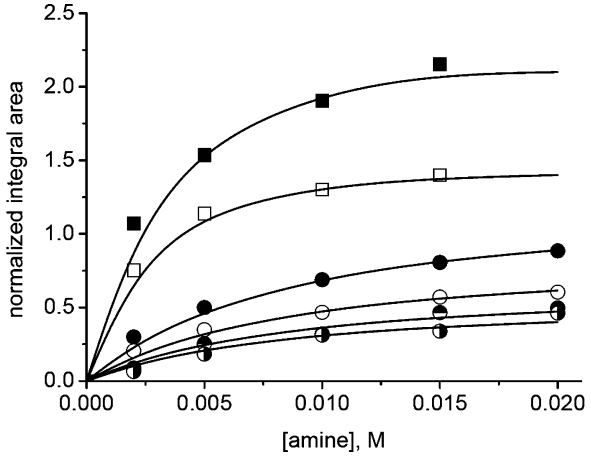

Figure 5. Integrated intensities of the signals arising from **2** (circles: ●, 3.1 ppm; ○, 2.9 ppm; ◑, 6.8 ppm; ◓, 7.1 ppm), **9** (■, 3.0 ppm), and **10** (□, 3.0 ppm) in NOE-pumping experiments with **1**-AuNP, as a function of the analyte concentration. Solid line: best fit of the data. Conditions: [AuNP] = 29 μM.

diamines with one (1:1) or two (1:2) crown ether moieties on the nanoparticle surface. Good fits are obtained by postulating both a 1:1 ($K_{assoc} = 6.2 \times 10^2$ M^{-1} for **9** and 9.9×10^2 M^{-1} for **10**) and 1:2 ($K_{assoc} = 4.5 \times 10^2$ M^{-1} for **9** and 6.3×10^2 M^{-1} for **10**) interaction.[28] The evidence of an almost identical affinity of the nanoparticles for the two diamines is not surprising, since the flexibility of the substrates and of thiol **1** allows them to find the conformation most suitable for the recognition event. The binding strengths of diamines are in any case larger than those obtained for **2**, supporting the occurrence of a 1:2 interaction. Indeed, when the titration experiments were repeated using **9** and **10** in the monoprotonated form, binding constant values were very close to those obtained for **2** (see Figure S15). Such observations suggest that the

DOI: 10.1021/jacs.5b06300
J. Am. Chem. Soc. 2015, 137, 11399−11406

protonated diamines can simultaneously bind two crown ether moieties on the particle surface and such ditopic interaction results in a stronger affinity. On the other hand, when only one of the two amino groups is protonated, ditopic binding is not possible anymore, and the affinity for the nanoparticles drops to the values observed for protonated monoamines.

Closer inspection of Figure 5 reveals also that the sensitivity of the detection system for **2**, **9**, and **10** is quite different. Indeed, the signals obtained in the NOE pumping experiments for the diamines, when saturation binding is reached, are 2−4 times more intense than those produced with **2**. As a consequence of this effect and of the higher affinity, the detection limit of **9** and **10** decreases to 0.4 and 0.7 mM, respectively.[27]

The intensity of the substrate signal recorded in the NOE pumping experiment depends on four main parameters: the amount of substrate bound to the nanoparticle, its mean residence time, the local mobility of the substrate inside the monolayer, and the spatial proximity between the substrate and receptors spins. Once saturation is reached, no difference is expected between mono- and diamines regarding the amount of substrate bound. Hence, the greater sensitivity for protonated diamines likely arises from the other three factors at play, which all favor a ditopic binding mode. Indeed, the substrate residence time in the nanoparticle monolayer is expected to be longer in the case of 1:2 binding, since dissociation requires a simultaneous detachment of two ammonium groups. Also, the local mobility is expected to be reduced by the two-point interaction, increasing the extent of NOE magnetization transfer. Moreover, the ditopic binding mode would likely result in a greater spatial proximity between the spins of the substrate and those of the crown ether moiety.

The larger affinity and sensitivity for diamines with respect to monoamines should result in selective detection of the former. This hypothesis was verified by a competition experiment performed with tyramine (**2**) and putrescine (**9**) hydrochlorides (Figure 6) as target analytes. In this case, the signals arising from **9** are clearly visible in the NOE pumping spectra, while those from **2** are virtually undetectable.

Having defined the main features of the detection systems, we decided to investigate its ability to detect other relevant polyamines. Indeed, multivalent binding should lead to greater affinity, and consequently sensitivity, as the number of ammonium groups interacting with **1** units on the nanoparticle surface is increased.

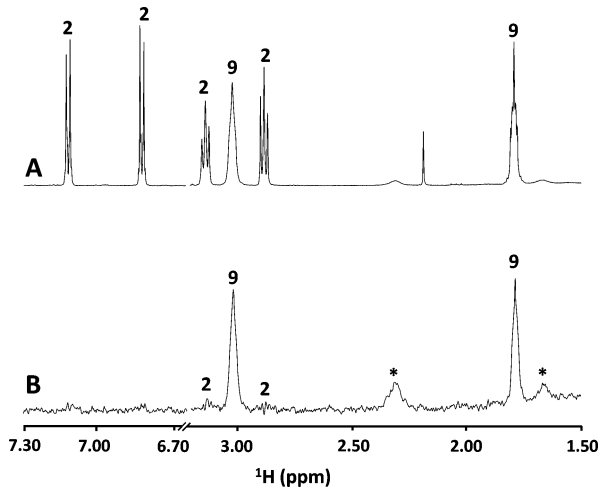

Figure 6. (A) ^{1}H NMR spectrum of **2** and **9** (10 mM in CD_3OD). (B) NOE pumping spectrum of **2** and **9** in the presence of **1**-AuNP (29 μM) (* = nanoparticles' residual signal).

NMR chemosensing performed with **1**-AuNP was able to detect spermine hydrochloride **11** in CD_3OD/D_2O 98.5:1.5[29] with an estimated limit of detection of 1 mM (Figure S8). Such a sensitivity, similar to that found for protonated diamines **9** and **10**, is justified by the fact that only two out of four amino groups in **11** are primary and effectively interact with the crown ether moieties. This hypothesis is supported by the fact that tris(2-aminoethyl)amine hydrochloride (TREN) **12**, which features three primary ammonium groups, is detected in CD_3OD/D_2O 99.4:0.6 with a K_{assoc} value of 2.4×10^3 M^{-1} (postulating a 1:3 interaction) and a limit of detection of 0.3 mM (Figure S10).

As a final test, we decided to investigate the effectiveness of the sensing system in water. It is well-known that the binding constants of crown ethers for ammonium ions are usually 2 orders of magnitude lower in water than in methanol.[20] Nonetheless, NMR chemosensing performed with **1**-AuNP in D_2O (buffered with 10 mM HEPES at pD 7.5) could detect both tyramine **2** and putrescine **9** at 10 mM concentration (Figure S9).

Guidelines for the Design of NMR Chemosensors. On the basis of the results discussed here and in our previous reports,[17] it is possible to define the main requirements that a nanoparticle-based receptor must fulfill to effectively perform as an NMR chemosensor.

Regarding the structure and the functionalization of the nanoparticle, the main points to consider are (1) the nanoparticle size, (2) the functionalization density, and (3) the length of the spacer chain. The nanoparticle size must be large enough to let the diffusion filter dephase the magnetization of the small molecules while preserving that of the nanoparticles. As an example, in order to retain 80% of the nanoparticle magnetization and only 1% of the analyte magnetization, the nanoparticle diffusion rate must be at least 20 times larger than that of the analytes. On the other hand, the length and flexibility of the coating molecules must be large enough to let their magnetization survive up to the beginning of NOE magnetization transfer. Still, too flexible coating molecules will produce signals with long T_2 values that will not be efficiently removed by the CPMGz filter.[16a]

The best compromise depends on the diffusion rate of the analytes to detect and on the chemical structure of the coating molecules. In the case of analytes with molecular weights below 300 Da, gold nanoparticles with a 2 nm gold core coated with a monolayer of molecules about 10−20 atoms long nicely fulfill this requirement. Larger nanoparticles will be characterized by larger rotational correlation times τ_c and by shorter relaxation times.[30] Consequently, nanoparticles with a gold core diameter larger than 4 nm should not be used, unless the ligand length is sensibly increased and the binding occurs in the outer region of the ligand shell.

The density of receptor units on the nanoparticle surface must be optimized taking two factors into account. First, as suggested by the results discussed earlier, a high density of receptors on the nanoparticle surface may produce a steric hindrance that reduces their affinity for the analyte. Second, an effective detection requires a binding geometry such that the spins of the analyte and of the nanoparticle are close enough for NOE magnetization transfer.

DOI: 10.1021/jacs.5b06300
J. Am. Chem. Soc. 2015, 137, 11399−11406

The second point to analyze is the affinity of the receptor for the analyte and the role of the residence time. The influence of the binding affinity on the detection limit has already been discussed in a previous paper.[17b] In order to be effective, the mean residence time of the substrate in the bound state should be larger than the nanoparticle τ_c, while keeping the system in the fast exchange regime. If $\tau_c \sim 10$ ns and the spins are set 4 ppm apart at 500 MHz proton Larmor frequency, then $10^3 \ll k_{off} \ll 10^8$ s^{-1}. In the case of an association rate (k_{on}) close to the diffusion limit of 10^{10} M^{-1} s^{-1} (as in the case of crown ethers),[31] binding constants in the range 10^2–10^7 M^{-1} would be suitable, being $K_{assoc} = k_{on}/k_{off}$. Smaller k_{on} values will consequently reduce the maximum acceptable affinity. Indeed, large binding constants and low complex formation rates will lead to very high residence times, which turn into a decrease of the analyte diffusion coefficient and a less efficient NOE or diffusion filtration (Scheme 1).

CONCLUSION

In the end, the overall picture that emerges from the experiments reported here is stimulating: conjugation of crown ether derivatives with monolayer protected nanoparticles is a straightforward strategy to create chemosensors for protonated organic primary amines. Moreover, at difference from 18-crown-6, **1**-AuNP binds diamines with a greater affinity than monoamines, due to the spontaneous formation of ditopic binding sites. The self-organization of the binding units on the nanoparticle surface hence results in the formation of more complex binding sites, and in a change of the system selectivity with respect to the parent receptor. This produces an NMR chemosensor capable of detecting biogenic diamines with a submillimolar detection limit both in methanol and in water.

The most relevant feature is however the possibility to unambiguously identify the analyte and even to discriminate between homologues differing by a single methylene residue in the alkyl chain. Such an ability is precluded to most supramolecular chemosensors, since the signal triggered by the recognition event results from the modulation of a receptor-related property. Indeed, the intensity of the generated signal contains the information on the amount of analyte present, but the information on the analyte identity rests upon trusting in the selectivity of the receptor. On the contrary, in the "NMR chemosensing" approach, the signal is produced by the substrate itself and contains all the information on an NMR spectrum, allowing both the discrimination and identification of very similar substrates which may bind to the receptor in a similar way.

In principle, the approach outlined here can be extended to any supramolecular receptor, thus providing a very general transduction mechanism for the development of new chemosensors. Combined NMR and chemical strategies are currently underway in our laboratories to improve the selectivity and sensitivity of the proposed method.[32]

ASSOCIATED CONTENT

Supporting Information

The Supporting Information is available free of charge on the ACS Publications website at DOI: 10.1021/jacs.5b06300.

Synthesis and characterization of **1** and **1**-AuNP, pulse sequences and experimental details, and additional NMR experiments (PDF)

AUTHOR INFORMATION

Corresponding Authors

*federico.rastrelli@unipd.it

*fabrizio.mancin@unipd.it

Present Address

†M.-V.S.: Laboratoire de Chimie des Biomolécules et de l'Environnement - CRIOBE - USR 3278 CNRS EPHE UPVD, Université de Perpignan Via Domitia (UPVD), 52 avenue Paul Alduy 66860 Perpignan, France.

Author Contributions

‡M.-V.S., G.S.: These authors contributed equally.

Notes

The authors declare no competing financial interest.

ACKNOWLEDGMENTS

This work was supported by the Starting Grants Project MOSAIC 259014 granted to F.M. by ERC and PRAT CPDA 132473/13 granted to F.R. by Università degli Studi di Padova. This manuscript is dedicated to the memory of Prof. Alessandro Bagno.

REFERENCES

(1) Selected reviews: (a) *Fluorescent Chemosensors for Ion and Molecule Recognition*; Czarnik, A. W., Ed.; ACS Symposium Series 538; American Chemical Society: Washington, DC, 1993. (b) de Silva, A. P.; Gunaratne, H. Q. N.; Gunnlaugsson, T.; Huxley, A. J. M.; McCoy, C. P.; Rademacher; Rice, T. E. *Chem. Rev.* **1997**, *97*, 1515–1566. (c) Bissell, R. A.; De Silva, A. P.; Gunaratne, H. Q. N.; Lynch, P. L. M.; Maguire, G. E. M.; Sandanayake, K. *Chem. Soc. Rev.* **1992**, *21*, 187–195. (d) Xu, Z.; Chen, X.; Kim, H. N.; Yoon, J. *Chem. Soc. Rev.* **2010**, *39*, 127–137. (e) Oton, F.; Tarraga, A.; Espinosa, A.; Velasco, M. D.; Molina, P. *J. Org. Chem.* **2006**, *71*, 4590–4598. (f) McRae, R.; Bagchi, P.; Sumalekshmy, S.; Fahrni, C. J. *Chem. Rev.* **2009**, *109*, 4780–4827.

(2) Hulanicki, A.; Glab, S.; Ingman, F. *Pure Appl. Chem.* **1991**, *63*, 1247–1250.

(3) (a) Santos-Figueroa, L. E.; Moragues, M. E.; Climent, E.; Agostini, A.; Martinez-Manez, R.; Sancenon, F. *Chem. Soc. Rev.* **2013**, *42*, 3489–3613. (b) Albelda, M. T.; Frias, J. C.; Garcia-Espana, E.; Schneider, H. J. *Chem. Soc. Rev.* **2012**, *41*, 3859–3877. (c) Chen, X. Q.; Tian, X. Z.; Shin, I.; Yoon, J. *Chem. Soc. Rev.* **2011**, *40*, 4783–4804. (d) Lippert, A. R.; De Bittner, G. C. V.; Chang, C. J. *Acc. Chem. Res.* **2011**, *44*, 793–804. (e) Germain, M. E.; Knapp, M. J. *Chem. Soc. Rev.* **2009**, *38*, 2543–2555. (f) Mills, A. *Chem. Soc. Rev.* **2005**, *34*, 1003–1011.

(4) Mancin, F.; Rampazzo, E.; Tecilla, P.; Tonellato, U. *Chem. - Eur. J.* **2006**, *12*, 1844–1854.

(5) (a) Chen, K.; Shu, Q. H.; Schmittel, M. *Chem. Soc. Rev.* **2015**, *44*, 136–160. (b) Li, X. H.; Gao, X. H.; Shi, W.; Ma, H. M. *Chem. Rev.* **2014**, *114*, 590–659. (c) Vargas Jentzsch, A.; Hennig, A.; Mareda, J.; Matile, S. *Acc. Chem. Res.* **2013**, *46*, 2791–2800. (d) Chan, J.; Dodani, S. C.; Chang, C. J. *Nat. Chem.* **2012**, *4*, 973–984. (e) Kobayashi, H.; Longmire, M. R.; Ogawa, M.; Choyke, P. L. *Chem. Soc. Rev.* **2011**, *40*, 4626–4648.

(6) Grynkiewicz, G.; Poenie, M.; Tsien, R. Y. *J. Biol. Chem.* **1985**, *260*, 3440–3450.

(7) (a) Gunnlaugsson, T.; Glynn, M.; Tocci, G. M.; Kruger, P. E.; Pfeffer, F. M. *Coord. Chem. Rev.* **2006**, *250*, 3094–3117. (b) de Silva, A. P.; Moody, T. S.; Wright, G. D. *Analyst* **2009**, *134*, 2385–2393. (c) de Silva, A. P. *Isr. J. Chem.* **2011**, *51*, 16–22.

(8) (a) McFarland, S. A.; Finney, N. S. *J. Am. Chem. Soc.* **2001**, *123*, 1260–1261. (b) Chen, C.-T.; Wagner, H.; Still, W. C. *Science* **1998**, *279*, 851–853.

(9) (a) Zheng, J.; Yang, R. H.; Shi, M. L.; Wu, C. C.; Fang, X. H.; Li, Y. H.; Li, J. H.; Tan, W. H. *Chem. Soc. Rev.* **2015**, *44*, 3036–3055. (b) Tjong, V.; Tang, L.; Zauscher, S.; Chilkoti, A. *Chem. Soc. Rev.*

DOI: 10.1021/jacs.5b06300
J. Am. Chem. Soc. 2015, 137, 11399–11406

2014, *43*, 1612−1626. (c) Krishnan, Y.; Simmel, F. C. *Angew. Chem., Int. Ed.* **2011**, *50*, 3124−3156.
(10) (a) Ghale, G.; Nau, W. M. *Acc. Chem. Res.* **2014**, *47*, 2150−2159. (b) Nguyen, B. T.; Anslyn, E. V. *Coord. Chem. Rev.* **2006**, *250*, 3118−3127. (c) Wiskur, S. L.; Ait-Haddou, H.; Lavigne, J. J.; Anslyn, E. V. *Acc. Chem. Res.* **2001**, *34*, 963−972.
(11) Plaunt, A. J.; Clear, K. J.; Smith, B. D. *Chem. Commun.* **2014**, *50*, 10499−10501.
(12) Xie, X. J.; Bakker, E. *Anal. Bioanal. Chem.* **2015**, *407*, 3899−3910.
(13) (a) Que, E. L.; Domaille, D. W.; Chang, C. J. *Chem. Rev.* **2008**, *108*, 1517−1549. (b) McRae, R.; Bagchi, P.; Sumalekshmy, S.; Fahrni, C. J. *Chem. Rev.* **2009**, *109*, 4780−4827. (c) Haas, K. L.; Franz, K. J. *Chem. Rev.* **2009**, *109*, 4921−4960.
(14) (a) Zhao, Y.; Swager, T. M. *J. Am. Chem. Soc.* **2013**, *135*, 18770−18773. (b) Zhao, Y.; Markopoulos, G.; Swager, T. M. *J. Am. Chem. Soc.* **2014**, *136*, 10683−1069. (c) Zhao, Y.; Swager, T. M. *J. Am. Chem. Soc.* **2015**, *137*, 3221−3224.
(15) For other recently reported methods for NMR detection and identification of compounds in mixtures, see ref 11 and: Kitamura, M.; Suzuki, T.; Abe, R.; Ueno, T.; Aoki, S. *Inorg. Chem.* **2011**, *50*, 11568−11580 and references therein..
(16) (a) Rastrelli, F.; Jha, S.; Mancin, F. *J. Am. Chem. Soc.* **2009**, *131*, 14222−14223. (b) Guarino, G.; Rastrelli, F.; Mancin, F. *Chem. Commun.* **2012**, *48*, 1523−1525. (c) Guarino, G.; Rastrelli, F.; Scrimin, P.; Mancin, F. *J. Am. Chem. Soc.* **2012**, *134*, 7200−7203.
(17) (a) Perrone, B.; Springhetti, S.; Ramadori, F.; Rastrelli, F.; Mancin, F. *J. Am. Chem. Soc.* **2013**, *135*, 11768−11771. (b) Salvia, M.-V.; Ramadori, F.; Springhetti, S.; Diez-Casellnou, M.; Perrone, B.; Rastrelli, F.; Mancin, F. *J. Am. Chem. Soc.* **2015**, *137*, 886−892.
(18) Chen, A.; Shapiro, M. J. *J. Am. Chem. Soc.* **1998**, *120*, 10258−10259.
(19) For other examples of crown ether functionalized nanoparticles for sensing, see: (a) Lin, S.-Y.; Wu, S.-H.; Chen, C.-h. *Angew. Chem., Int. Ed.* **2006**, *45*, 4948−4951. (b) Russell, L. E.; Pompano, R. R.; Kittredge, K. W.; Leopold, M. C. *J. Mater. Sci.* **2007**, *42*, 7100−7108. (c) Patel, G.; Kumar, A.; Pal, U.; Menon, S. *Chem. Commun.* **2009**, 1849−1851. (d) Kuang, H.; Chen, W.; Yan, W.; Xu, L.; Zhu, Y.; Liu, L.; Chu, H.; Peng, C.; Wang, L.; Kotov, N. A.; Xu, C. *Biosens. Bioelectron.* **2011**, *26*, 2032−2037. (e) Velu, R.; Ramakrishnan, V. T.; Ramamurthy, P. *Tetrahedron Lett.* **2010**, *51*, 4331−4335.
(20) See: (a) Izatt, R. M.; Lamb, J. D.; Izatt, N. E.; Rossiter, B. E.; Christensen, J. J.; Haymore, B. L. *J. Am. Chem. Soc.* **1979**, *101*, 6273−6276. (b) Rudiger, V.; Schneider, H. J.; Solov'ev, V. P.; Kazachenko, V. P.; Raevsky, O. A. *Eur. J. Org. Chem.* **1999**, *1999*, 1847−1856. (c) Buschmann, H. J.; Mutihac, L.; Jansen, K. *J. Inclusion Phenom. Mol. Recognit. Chem.* **2001**, *39*, 1−11. (d) Spath, A.; Konig, B. *Beilstein J. Org. Chem.* **2010**, *6*, 1−111.
(21) (a) Jana, N. R.; Peng, X. *J. Am. Chem. Soc.* **2003**, *125*, 14280−14281. (b) Manea, F.; Bindoli, C.; Polizzi, S.; Lay, L.; Scrimin, P. *Langmuir* **2008**, *24*, 4120−4124.
(22) Nanoparticle concentration can be converted into concentration of **1** units by multiplying it by 75, with the average nanoparticle formula being $Au_{180}RS_{75}$ (Supporting Information). In this study, nanoparticle concentration was not optimized.
(23) Neuhaus, D.; Williamson, M. *The nuclear Overhauser effect in structural and conformational analysis*; VCH: 1989.
(24) Compound **4** features a protonated secondary amine and as such can form only two hydrogen bonds with the 18-crown-6 moiety, resulting in a lower affinity of the crown ether receptor, see ref 20d.
(25) In our previous paper (ref 17a), we indicated STD as an alternative method for nanoparticle-assisted NMR detection, featuring a better sensitivity at the expense of a reduced general applicability. Results reported here confirm this picture. STD based NMR chemosensing results in higher signal-to-noise rations but suffers from signal overlaps.
(26) See, for example: Dunbar, A. D. F.; Richardson, T. H.; McNaughton, A. J.; Hutchinson, J.; Hunter, C. A. *J. Phys. Chem. B* **2006**, *110*, 16646−16651.
(27) The detection limit reported is relative to the experimental condition detailed in the Supporting Information. Instrumental apparatus and experimental conditions may lead to relevant sensitivity improvements.
(28) Fittings were performed using a 1:1 binding model where the concentration of binding sites was fixed respectively at the nominal concentration of 1 units (1:1) or at its half (1:2).
(29) A small amount of D_2O was added to ensure full solubility of the amine salts.
(30) Hostetler, M. J.; Wingate, J. E.; Zhong, C.-J.; Harris, J. E.; Vachet, R. W.; Clark, M. R.; Londono, J. D.; Green, S. J.; Stokes, J. J.; Wignall, G. D.; Glish, G. L.; Porter, M. D.; Evans, N. D.; Murray, R. W. *Langmuir* **1998**, *14*, 17−30.
(31) Adamic, R. J.; Lloyd, B. A.; Eyring, E. M.; Petrucci, S.; Bartsch, R. A.; Pugia, M. J.; Knudsen, B. E.; Liu, Y.; Desai, D. H. *J. Phys. Chem.* **1986**, *90*, 6571−6576.
(32) Salvia, M. V.; Salassa, G.; Gabrielli, L.; Springhetti, S.; Rosa Gastaldo, D.; Trevisan, L.; Rastrelli, F.; Mancin, F. Patent application PD102015000040417 (30/7/2015).

DOI: 10.1021/jacs.5b06300
J. Am. Chem. Soc. 2015, 137, 11399−11406